Carbohydrate Polymers 86 (2011) 644–651

Contents lists available at ScienceDirect

Carbohydrate Polymers

journal homepage: www.elsevier.com/locate/carbpol

Temperature and time effects on the structural properties of a non-aqueous ethyl cellulose topical drug delivery system

Lilia Bruno [a], Stefan Kasapis [b,*], Vinita Chaudhary [b], Keat Theng Chow [c], Paul W.S. Heng [c], Lai Peng Leong [a]

[a] Department of Chemistry, National University of Singapore, Block S8, Level 3, Science Drive 3, Singapore 117543, Singapore
[b] School of Applied Sciences, RMIT University, City Campus, Melbourne Vic 3001, Australia
[c] Department of Pharmacy, National University of Singapore, 18 Science Drive 4, Singapore 117543, Singapore

ARTICLE INFO

Article history:
Received 26 March 2011
Received in revised form 10 April 2011
Accepted 2 May 2011
Available online 7 May 2011

Keywords:
Ethyl cellulose
Propylene glycol dicaprylate
Non-aqueous gel
Time–temperature superposition

ABSTRACT

The structural properties of ethyl cellulose and propylene glycol dicaprylate mixtures were investigated with a view to facilitating use of the system as excepient for topical drug delivery. The working protocol included small-deformation dynamic oscillation in combination with the principle of time–temperature superposition, micro and modulated differential scanning calorimetry, wide-angle X-ray diffraction patterns, infrared spectroscopy, and optical profile analysis in the form of gel particle roughness. In contrast to thermoreversible gelation upon heating of aqueous ethyl cellulose solutions reported widely in the literature, replacing water with propylene glycol dicaprylate and mixing with the polymer yields gels that revert to the solution state with increasing temperature. Time effects were also probed; the continuous increase in viscoelasticity of preparations as a function of time of observation at ambient temperature was accompanied by structural disintegration of the polymeric particles. This was rationalized by proposing that specific polymer–solvent interactions result with aging in particle erosion and the release of polymeric strands that are able to form a three-dimensional structure. It was thus documented that the time–temperature equivalence was active in the system producing a rubbery state in the master curve of viscoelasticity, which extends from ambient to subzero temperatures and should facilitate pharmaceutical applications.

1. Introduction

Cellulose derivatives are commonly ethers of alkyl or hydroxyalkyl groups substituted in part on the three available hydroxyl groups of each anhydroglucose unit in the cellulose chain. Substitution results in disorder, which spreads apart the polymeric segments so that an aqueous or organic solvent may solvate them. Thus, the degree and type of substitution will dictate a broad range of functional characteristics in aqueous/non-aqueous preparations with industrial application (Stenstad, Andresen, Tanem, & Stenius, 2008; Ziegler, Tanczos, Horvolgyi, & Agoston, 2008). Prior to dealing with the gelation of hydrophobically substituted polysaccharides, it should be mentioned that the mechanism of their cold-set hydrophilic counterparts, for example, agarose, carrageenans, deacylated gellan and gelatin, is fairly well understood (Raimo, 2007; Tanaka, Gong, & Osada, 2005). Furthermore, the availability of hydrophilic gelling agents resulted in a plethora of studies on aqueous gels, as compared to the non-aqueous systems (Janaswamy and Chandrasekaran, 2005; Nishinari and Zhang, 2004).

The origin of associations of apolar-substituent polymers in an aqueous solvent is determined by the balance of an increase in entropy (positive ΔS) and a decrease in enthalpy (negative ΔH) effecting changes in the Gibbs free energy (ΔG) as a function of temperature. In the case of aqueous ethyl cellulose systems, an extrapolation can be made from solid clathrates (hydrophobic hydrates), in which hydrocarbon moieties are trapped and free to rotate within a hydrogen-bonded cage of water molecules (Yoon et al., 2008). Increasing the temperature of the system is entropically very unfavorable as it imposes a degree of strain in the freedom of water molecules whose "ordered" arrangements become increasingly less stable on heating (Haque and Morris, 1993). Eventually, a temperature is reached where the apolar residues of the polymer are withdrawn from aqueous contact and the structured water is released, causing an increase in entropy. The exposed hydrophobic groups bind now into associations with other hydrophobic groups of neighboring molecules (Wang, Dong, & Xu, 2007). This is enthalpically costly but the hydrophobic interaction is a partial reversal of the entropically unfavorable hydration process, with this hydrophobic interaction being the dominating factor leading to high-temperature gelation (Tanaka and Koga, 2000).

* Corresponding author. Tel.: +61 3 9925 5244; fax: +61 3 9925 7110.
E-mail address: stefan.kasapis@rmit.edu.au (S. Kasapis).

0144-8617/$ – see front matter © 2011 Published by Elsevier Ltd.
doi:10.1016/j.carbpol.2011.05.002

Details of the gelation mechanism appear to be heavily governed by the substitution pattern or functional group, and in the case of a regioselectively substituted 3-*O*-methoxyethyl cellulose there is very little in the dynamic oscillatory spectrum to suggest structure formation upon heating (Sun et al., 2009).

Besides considerations of structure formation in water, non-aqueous solvents are of increasing interest since they can be used as vehicle for topical drug delivery (Qiu and Bae, 2006). Water poses a risk of hydrolytic reactions and the alternative formulations of hydroalcoholic compounds (e.g., ethanol) can neither eliminate the possibility of drug hydrolysis nor prevent undesirable variation in formulation owing to high evaporative potential (Agrawal, Manek, Kolling, & Neau, 2003). An example of a carrier that can improve chemical stability of moisture sensitive drugs is the non-aqueous ethylcellulose matrix that is able to structure the hydrophobic solvent. Ethyl cellulose (EC) has found application as a polymeric coating, in controlled release of oral dosage forms, in transdermal films and patches, and as a particulate emulsion stabilizer (Arora and Mukherjee, 2002; Li, Kresse, Xu, & Springer, 2001; Melzer, Kreuter, & Daniels, 2003; Wu, Huang, Chang, Tsai, & Tsai, 2003). Unpublished results of this research group have demonstrated that a formulation containing EC, the non-volatile solvent of propylene glycol dicaprylate/dicaprate (PGD), and low levels of minocycline hydrochloride (0.05% w/w) provided satisfactory antibacterial activity against *Propionibacterium acnes*, as compared to a blank gel matrix and a standard minocycline hydrochloride solution.

Research efforts have been directed into formulating topical dosage forms possessing physicochemical and aesthetic criteria that ensure clinical efficacy and patient acceptability. The physical properties relevant to topical applications of non-aqueous EC gels have been characterized in several reported studies. However, fundamental understanding of the EC polymer properties in non-aqueous systems is still scarce in the literature. Formation of clear and thermoreversible gels had been reported upon cooling of EC/diester phthalate solutions (Lizaso, Munoz, & Santamaria, 1999). Thixotropic gels with an extended linear viscoelastic region that exhibit desirable wetting behaviour in their function as a moisture barrier were produced with 11–16% (w/w) EC in the formulation at various particle grades (Chan, Chow, & Heng, 2006; Heng, Chan, & Chow, 2005). Blends of EC with poly(propylene carbonate) exhibited a range of viscoelastic consistencies from predominantly amorphous regions to cholesteric liquid crystalline structures in the rich EC composition range (Zhang et al., 2006). We felt that a study on the molecular characteristics of EC in non-aqueous PGD will go a long way to fill in gaps associated with the functionality of these systems in pharmaceutical applications relevant to topical drug delivery.

2. Materials and methods

2.1. Materials

The industrial ethyl cellulose sample used in this study was a water-insoluble, thermoplastic cellulose ether with a randomly substituted pattern and a white powder appearance. The supplier provided data of the ethoxy content of the polymer and degree of substitution (d.s.), which are 49.0 ± 0.5% and about 2.6, respectively (Ethocel Std 100 FP Premium EC100 supplied by Dow Chemical, Midland, MI). Our characterisation work produced the following: Glass transition temperature of the powder is 131 ± 2 °C and the material remains stable up to its melting point (~165 °C). Molecular weights, M_w and M_n (g/mol), and polydispersity, M_w/M_n, of EC100 were obtained by gel permeation chromatography using Styragel column and a reflective index detector (Models 2690, 2410, Waters, Milford, MA) at 40 °C. Tetrahydrofuran was the mobile phase and polystyrene standards provided the calibration curve; details of this standard method to determine molecular weight data of ethyl cellulose samples can be found in the literature (Sanchez, Franco, Delgado, Valencia, & Gallegos, 2011). Results expressed as means from duplicated determinations are as follows: M_w = 130,270, M_n = 74,740, and M_w/M_n = 1.7, which are close to supplier's information.

The non-aqueous solvent used presently is a hydrophobic diester derivative of propylene glycol and it is commercially available by Sasol GmbH, Witten, Germany. The solvent is a non-volatile neutral oil exhibiting viscosity of about 10 mPa s at 20 °C with caprylic acid and capric acid contents of 65–80% and 20–35%, respectively (propylene glycol dicaprylate/dicaprate; Miglyol 840).

2.2. Gel preparation

To evaluate the structural properties of our systems, ethyl cellulose was mixed with propylene glycol dicaprylate/dicaprate (PGD) using continuous stirring at 300 rpm and ambient temperature for 15 min. This leads to the formation of a homogeneous gel and air bubbles were removed by applying vacuum. All material concentrations were expressed on a weight-per-weight basis (w/w).

2.3. Rheological measurements

Small deformation dynamic-oscillation measurements in shear were performed using AR-G2, a rheometer with a magnetic thrust bearing technology for nano-torque control (TA Instruments, New Castle, DE). The analysis provides readings of the storage modulus in shear (G') which is the elastic component of the network, loss modulus (G''; viscous component) and complex dynamic viscosity (η^*). Variations with time and temperature can further be assessed as a measure of the 'phase lag' δ ($\tan\delta = G''/G'$) of the relative liquid-like and solid-like structure of the material. Temperature control is achieved with a Peltier plate at a range between −30 and 120 °C and accuracy of ±0.1 °C. Experimental routines were carried out within the linear viscoelastic region (LVR) of the material loaded onto the parallel plates of the measuring geometry (40 mm diameter; 1.5 mm gap). These included successive temperature (heating/cooling) sweeps between 25 and 90 °C at a scan rate of 1 °C/min, frequency of 1 rad/s and strain of 0.5%, frequency sweeps from 0.1 to 100 rad/s at 0.5% strain, and time sweeps up to 9000 min at a frequency of 1 rad/s and strain of 0.5%.

2.4. Thermal analysis

Rheological work was complemented with differential scanning calorimetry using micro DSC (Setaram VII; SETARAM Instrumentation, Caluire, France) and modulated DSC (MDSC 2000; TA Instruments, New Castle, DE). In the former, approximately 300 mg of the gel was subjected to heating followed by a cooling cycle of 25–90–25 °C at 1 °C/min. This temperature range was extended using MDSC where 9 mg of the EC/PGD gel was subjected to cooling and heating routines between 25 and −80 °C at a rate of 5 °C/min. A modulated temperature-sweep mode was used with an oscillating period of 60 s and amplitude ±1 °C described previously (Kontogiorgos, Goff, & Kasapis, 2008), and the thermograms of total, reversing and non-reversing heat flow were examined in this study. Instrument calibration included a traceable indium standard and a sapphire standard.

2.5. X-ray diffraction studies

Wide-angle X-ray diffraction patterns of the EC/PGD gel were obtained using a SIEMENS D5005 X-ray Diffractometer (Bruker AXS, Karlsruhe, Germany) equipped with Cu Kα (1.54 Å) radiation. An accelerating voltage and current of 40 kV and 40 mA, respectively,

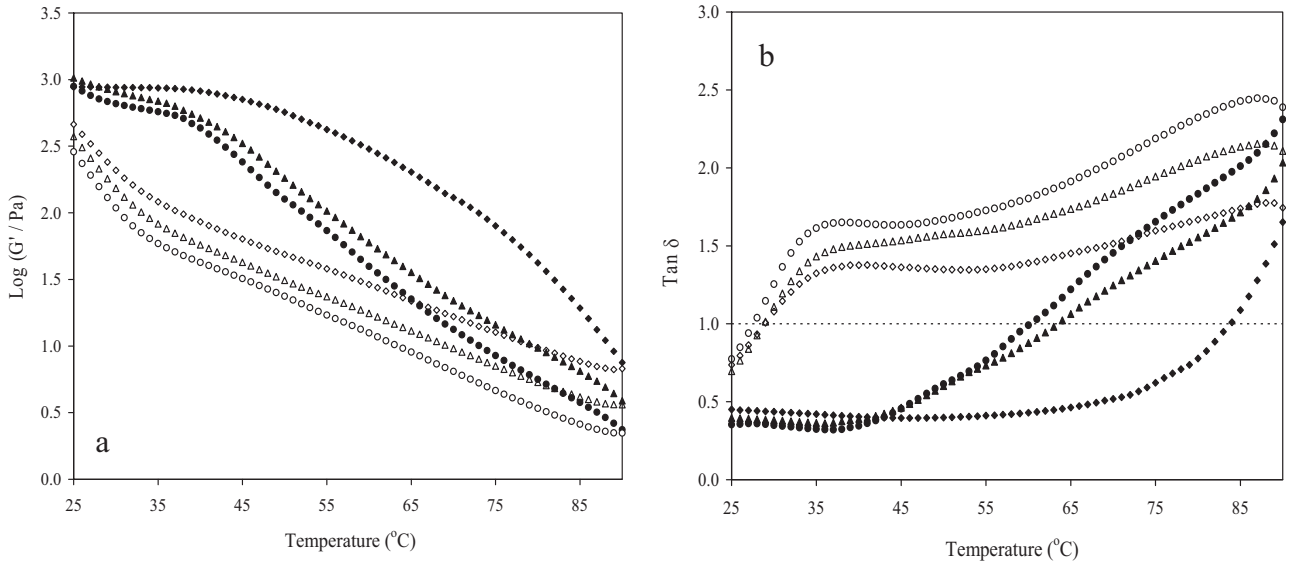

Fig. 1. Elastic modulus (a) and tan δ (b) obtained from controlled heating (closed symbols) and cooling (open symbols) at a rate of 1 °C/min on 12% fresh EC/PGD gel: first temperature sweep (♦; ◊), second temperature sweep following isothermal aging at 25 °C for 48 h (▲; △), and third temperature sweep (●; ○) following another isothermal aging period at 25 °C for 48 h (scan rate: 1 °C/min; frequency: 1 rad/s; strain: 0.5%).

in combination with a scan rate of 0.8 °C/min were employed. The diffractograms were recorded in a 2θ range between 2° and 90°, and subsequently analysed using the Bruker Advanced X-ray Solutions software, DIFFRAC^{plus} Evaluation (Eva), version 10.0 revision 1.

2.6. ATR-FTIR analysis

ATR-FTIR spectra of the EC/PGD gel were obtained using a Perkin Elmer One™ FTIR spectrometer equipped with MIRacle™ ZnSe single reflection ATR plate (Perkin-Elmer, Norwalk, CT). The spectrum of each material was finalized after averaging 200 scans between 4000 and 600 cm^{-1} with a resolution of 4 cm^{-1}. This was corrected against the background spectrum of the solvent at ambient temperature. Data acquisition was facilitated by the Spectrum v5.0.1 Software of Perkin-Elmer.

2.7. Optical profile analysis

Measurements of gel roughness were carried out with a Wyko NT1100 optical profile analyzer, which utilizes a scan area of 50×50 μm (Veeco, Tucson, AZ). Approximately 0.3 g of gel was spread on a flat surface (glass Petri dish), which was then mounted on the profile analyzer for scanning. Excess solvent present on the gel surface due to the capillary effect has a high tendency to result in an erroneously smooth surface (low roughness values). This effect was minimized by lining the Petri dish with filter paper to absorb excess solvent and by gently spreading the gel immediately prior to each measurement so that the structure within the bulk of the gel was captured in the scan. Scan rate for the acquisition of three dimensional images was 0.02°/min.

3. Results and discussion

3.1. Temperature course of mechanical properties in ethyl cellulose/propylene glycol dicaprylate mixtures

Mechanical properties of the non-aqueous EC/PGD system are monitored presently using small-deformation dynamic oscillation in shear. This approach possesses the advantage of preserving the delicate organization of the polymeric network as it forms. Prior to this, mechanical properties under increasing amplitude of oscillation were monitored to identify the linear viscoelastic region (LVR) of the material. The strain sweep showed that the solid-like response (G') dominated the liquid-like response (G''), with the former diminishing with increasing strain and falling finally below the G'' trace (data not shown). This pattern of behaviour produces an LVR region for the EC/PGD gel that extends to about 3.5% strain. An amplitude of deformation of 0.5% strain was chosen for subsequent experimentation in order to minimize the chance of network disruption whilst maintaining reasonable stress levels for an acceptable signal-to-noise ratio.

Mechanical spectra (i.e., variation of G', G'' and complex dynamic viscosity, η^*, as a function of frequency of oscillation, ω) were also recorded at ambient temperature (24 °C) within the experimental frequency range of 0.1–100 rad/s. Samples show evidence of gel-like character ($G' > G''$) with strong frequency dependence in the values of loss modulus. Thus the gap between the two modulus traces diminishes, with the values of tan δ increasing from 0.37 to 0.62 at the beginning and end of the frequency sweep, respectively (data not shown). Experimentation continued by following the changes in storage modulus and damping factor tan δ on heating and cooling of the EC/PGD gel at a controlled rate of 1 °C/min.

As shown in Fig. 1a, there is a gradual reduction in G' leading to material liquefaction, an outcome that is confirmed by the values of tan δ exceeding the threshold of one in Fig. 1b. This is, of course, in direct contrast to the process of association on heating often recorded as gel formation for aqueous preparations of randomly substituted methyl, hydroxylpropylmethyl and ethyl derivatives of cellulose described in Section 1 of this manuscript. Replacing water with PGD allows EC to restructure upon cooling but this requires a further isothermal run at 25 °C for 48 h for complete recovery thus making thermal hysteresis a notable feature in the molecular network dynamics.

Experiments with heating, cooling and an isothermal run were repeated twice to thoroughly ascertain the temperature induced properties of the material and, in doing so, it was observed that the first thermal profile was appreciably different from the rest. In cooling, for example, increase in the G' values is mostly gradual but is followed by a "second wave" of structure formation commencing at 34 °C. The involvement of two distinct molecular processes is also evident in the specific features of tan δ, which show a rapid reduction in the liquid-like component of the material towards

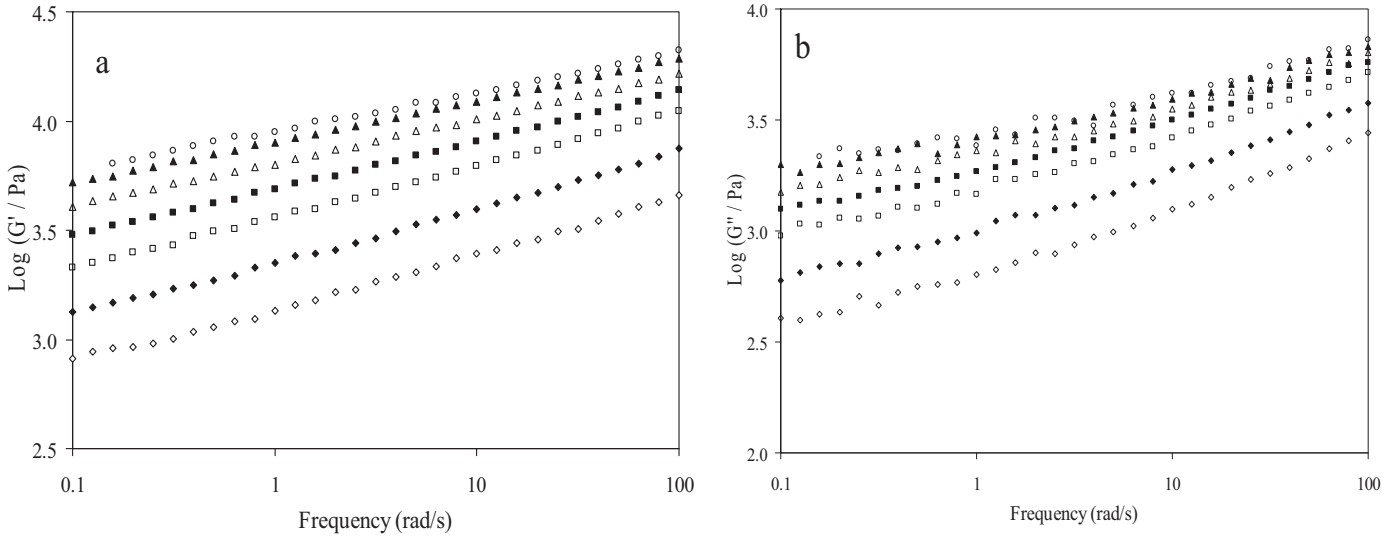

Fig. 2. Frequency variation of G' (a) and G'' (b) of a freshly made 12% EC gel in PGD at 5 (◊), 0 (♦), −5 (□), −10 (■), −15 (△), −20 (▲), and −25 °C (○).

completion of the cooling routine. The origin of this bimodal behaviour will be accounted for later, in discussions on the time course of structure formation in the EC/PGD gel.

Having considered the temperature dependence of molecular associations that give rise to structural variation of EC/PGD gels at temperatures in the range of ambient to 90 °C, we now attempt a complementary investigation at subzero temperatures. This was carried out by recording a series of standard mechanical spectra at regular temperature intervals of five degrees centigrade down to −25 °C. A typical sample of the results is reproduced for storage modulus in Fig. 2a and for loss modulus in Fig. 2b. Both moduli have relatively low values at higher temperature (e.g., 5 °C), whereas there is an order-of-magnitude build up of viscoelasticity at the low temperature end (i.e., −25 °C). Data was then processed following the method of reduced variable otherwise known as the time–temperature superposition principle (TTS) (Ferry, 1991; Kasapis, Al-Marhoobi, Deszczynski, Mitchell, & Abeysekera, 2003).

In doing so, a point was chosen arbitrarily as the reference temperature (T_o = −25 °C) and the remaining data were shifted along the log frequency axis until a uniform curve was obtained. In the absence of a phase transition, which would generate a non-reducible discontinuity in superposed data, a smooth variation in moduli at each experimental temperature reflects a change in state. This can be associated with a reference temperature following the horizontal superposition of data by a given shift factor. Fig. 3a depicts the master or composite curve obtained in this work for the EC/PGD gel, where the reduced moduli (G'_p and G''_p) cover a seven-decade frequency window. Good superposition of data argues for the validity of this approach monitoring a continuous relaxation of molecular dynamics in the system. Progress in viscoelasticity appears to establish an extended part of the "rubbery region" of the material, with the storage modulus being predominant and both traces showing a moderate frequency dependence according to synthetic polymer literature (Puscasu, Todd, Daivis, & Hansen, 2010).

Identical superposition of both modulus traces is a prerequisite for valid application of the method of reduced variables, thus yielding the shift factor (a_T) that integrates two sets of temperature data (T and T_o). The pattern of structural relaxation, as documented in the factor a_T for the horizontal superposition of mechanical spectra in Fig. 2a and b, is reproduced as a function of temperature in Fig. 3b. It was confirmed that the combined framework of Williams,

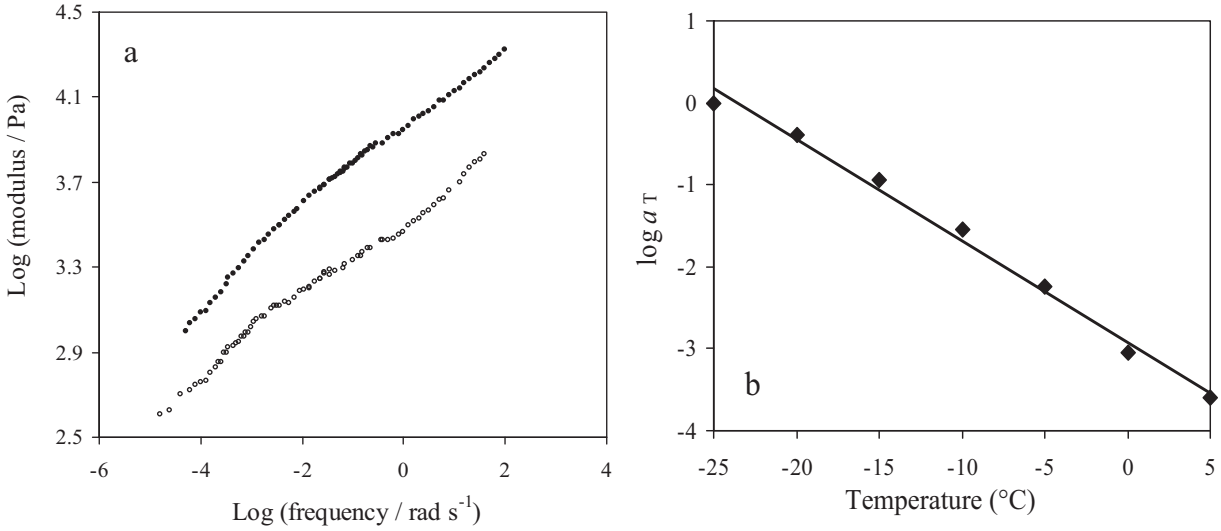

Fig. 3. (a) Composite curve of reduced shear moduli (G'_p (●); G''_p (○)) for the sample of Fig. 2 at the reference temperature of −25 °C, and (b) temperature variation of the factor a_T for the rubbery region (♦) of the sample, with the solid line reflecting the modified Arrhenius fit.

Landel, Ferry/free volume theory (Ferry, 1980) was unable to follow this progress in viscoelasticity, an outcome which argues for the absence of glass-transition related phenomena within the experimental temperature range of this investigation. Empirical rheology also indicates a rubbery state for the data in Fig. 3a, instead of a glassy consistency, as it pertains to oscillatory values of the complete dynamic-modulus function from the master curve of viscoelasticity (Alves, Mano, Gomez Ribelles, & Gomez Tejedor, 2004). However, the alternative framework of the reaction rate theory that translates to the following equation (Kasapis, 2008):

$$\log a_T = \frac{Ea}{2.303R}\frac{1}{T} - \frac{1}{To}$$

i.e., the modified Arrhenius equation achieves a good linear relationship ($r^2 = 0.992$) for the horizontal shift factor (R is the gas constant).

The constant activation energy (E_a) argues that relaxation processes in the rubbery region are heavily controlled by the specific chemical and conformational features of the material. The rubbery region reflects a timescale of observation in which there is no rearrangement of intermolecular associations ("entanglements" according to the theory of polymer viscoelasticity) but the configurational changes of chain segments between these associations are rapid. The modified Arrhenius equation provides an energetic-barrier estimate for a relaxation process relating to rearrangements beyond entanglements. Furthermore, the E_a value of 158 kJ/mol is comparable to estimates obtained for high-solid polysaccharide and glucose syrup preparations (98–140 kJ/mol) (Kasapis, 2001). This group of values contrasts strongly with the predictions of the reaction rate theory ($E_a = 0.47$ kJ/mol) for the rate of molecular diffusion of a bioactive compound (e.g., caffeine), which reflects the freedom of mobility of small organic molecules within, for example, an excepient carbohydrate matrix. The soft rubbery consistency of the EC/PGD preparation, as opposed to the hard and brittle properties of a glassy material, should ensure acceptable spreadability and absorption on the skin for drug delivery.

3.2. Time course of structural properties in ethyl cellulose/propylene glycol dicaprylate mixtures

Results thus far give a certain indication of the nature of molecular structures in the EC/PGD gel as affected by changing temperature. It is probable that besides temperature, holding the material isothermally over a period of time, which is accessible to normal laboratory operations, may further enhance our understanding of structural behaviour. A comparison with the temperature course of structural behaviour was attempted using an optical profile analyzer and recording gel roughness at ambient temperature. Fig. 4 reproduces the outcome of those changes over a prolonged period of observation (27 days) for untreated and thermally treated samples. The immediate observation is that the values of the root mean square roughness of the gel surface (R_q) of thermally treated gel samples are substantially lower than for the corresponding periods of observation in unheated materials indicating that the structural characteristics of the two systems are distinct.

There was an initial increase in the roughness values of freshly made samples ($R_q = 341 \pm 144.3$ nm), which culminated after three days of observation ($R_q = 467 \pm 138.7$ nm). This was followed by a sharp increase in light transmission (i.e., decrease in particle roughness) that reduced appreciably the size of measured entities following twenty seven days of observation ($R_q = 200.9 \pm 88.8$ nm). Overall, the relative magnitude of these changes argues for a time–temperature equivalence, which is qualitatively similar to the arguments deployed earlier in Figs. 2 and 3. It appears that under a longer period of observation (approximately thirty five days from the data in Fig. 4), both time and temperature treatments should yield comparable morphologies for the EC/PGD gel.

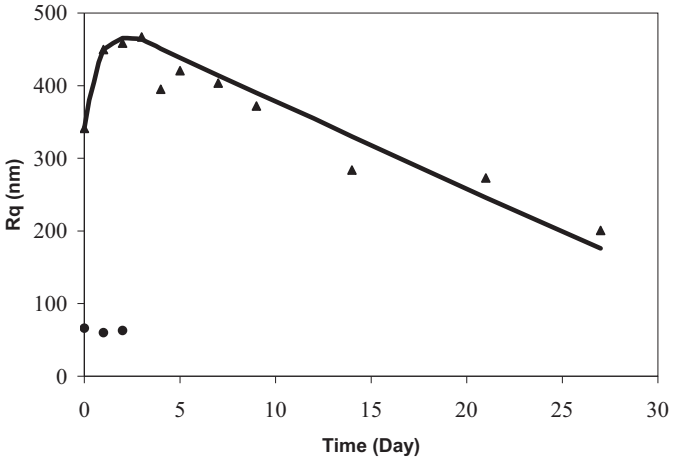

Fig. 4. Root mean square roughness (R_q) of the fresh (▲) and heated (●) 12% EC/PGD gel with respect to a time scale.

The partial disintegration of particle structure demonstrated with increasing time of observation in Fig. 4 is of interest but this trend was not apparent in similar isothermal routines that followed the mechanical properties of the preparation. As shown in Fig. 5, there is considerable increase in the values of storage and loss modulus in the initial stages of the time sweep, which is mirrored by the corresponding decrease in the damping factor, tan δ. At longer times, experimental traces level out thus achieving G' and tan δ values of 3.5 kPa and 0.28, respectively, after six days of continuous monitoring. That was the longest period of continuous experimentation allowed by the AR-G2 software, but subsequent implementation of frequency sweeps at regular time intervals of 24 h showed negligible development in moduli. Overall, results of this investigation demonstrated that the gelation process has reached a dynamic "pseudoequilibrium" as a function of time at a fixed temperature (25 °C).

3.3. Molecular interactions in ethyl cellulose/propylene glycol dicaprylate mixtures

A unifying theme in the discussion of Figs. 4 and 5 is that substantial proportion of the polymer is structurally mobile as

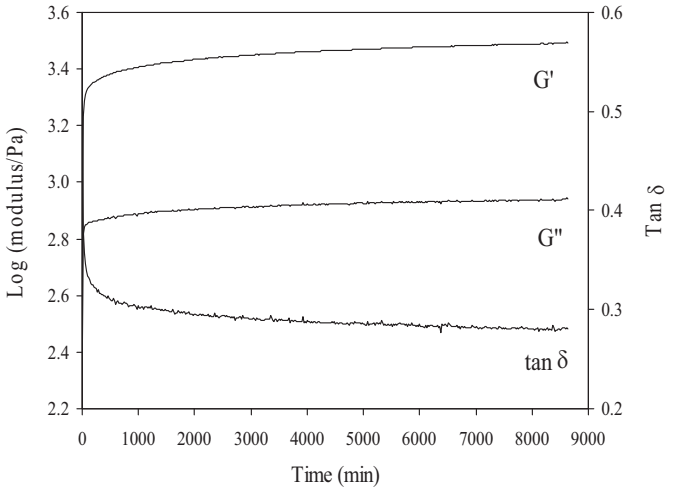

Fig. 5. Variation of storage modulus, loss modulus and tan δ as a function of time at 25 °C for 12% EC/PGD gel (frequency: 1 rad/s; strain: 0.5%).

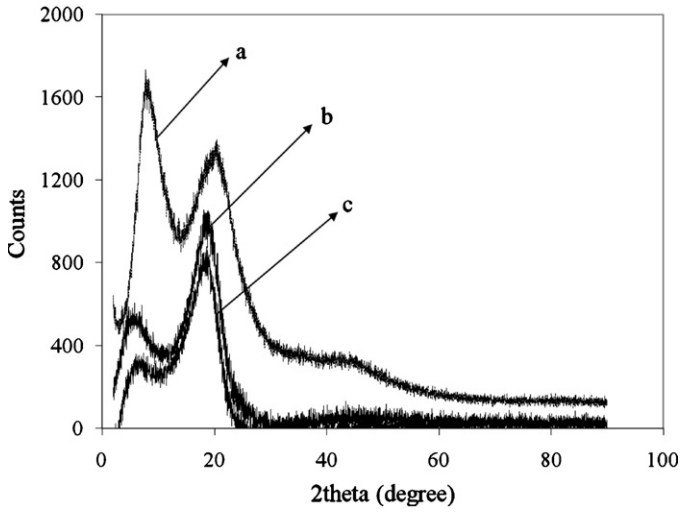

Fig. 6. Wide angle X-ray diffraction patterns for (a) ethyl cellulose powder, (b) freshly made gel of 12% EC in PGD, and (c) 12% EC/PGD gel undergone prior thermal treatment.

a function of time or temperature of observation, which indicates that ethyl cellulose interacts directly with the non-aqueous environment of propylene glycol dicaprylate. The nature of these molecular rearrangements and interactions was further pursued by monitoring the wide-angle X-ray diffraction patterns and ATR-FTIR spectra of our system. Fig. 6 offers a direct indication of the effect of the experimental protocol on the diffraction patterns of the cellulosic powder and the gel with or without thermal processing. In the former, diffraction peaks were observed at 2θ (°) of 8.4 and 20.6, an outcome that is characteristic of cholesteric liquid crystallinity (Huang, Ge, Li, & Hou, 2007). Furthermore, the small angle peak corresponds to the interlayer distance of the ordered chains of the polymer, with the second peak reflecting the interchain distance.

Together, the position of the two peaks indicates cellulose modification and generation of disorder in the system, with the projection of substituting groups along the axis being associated with an increase in the interfibrillar distance (Filho et al., 2007). Upon examination of the gel patterns, there is clear displacement of the diffraction peaks to smaller 2θ angles of 6.0 and 18.9, respectively, which suggests an increase in both the interlayer and interchain spacing due to polymer–solvent interactions in the gel. All along, the signal intensity of the X-ray patterns is reduced from the powder and the freshly made to the thermally treated gel as the conformational mobility of the polymeric backbone is augmented by the combined treatment of heating and solvent addition.

The effect of PGD solvent on ethyl substituted cellulose was also examined by using infrared spectroscopy and following the above line of approach in terms of preparing powdered samples and non-aqueous gels with or without thermal treatment. Fig. 7 reproduces the infrared spectra of the three samples following subtraction of the background signal from propylene glycol dicaprylate. A noticeable feature of the heated gel (spectrum *c*) is the peak at 1745 cm^{-1}, which is not present in EC powder and is relatively small in freshly made gels (spectra *a* and *b*, respectively). This outcome indicates that heat treatment facilitates molecular interactions between the carbonyl groups of the diester in the solvent and the hydroxyl groups of the polymer (Stenstad et al., 2008). Further insights into structural variations are afforded by the bands at 881 and 920 cm^{-1}, which are seen in the powdered sample but are below acceptable threshold values in spectra *b* and *c*. The former is characteristic of packing patterns of beta-glucan sequences with the latter being attributed to the stretching of out-of-plane rings of amorphous segments of the cellulose matrix (Panaitescu et al., 2007). Both are less

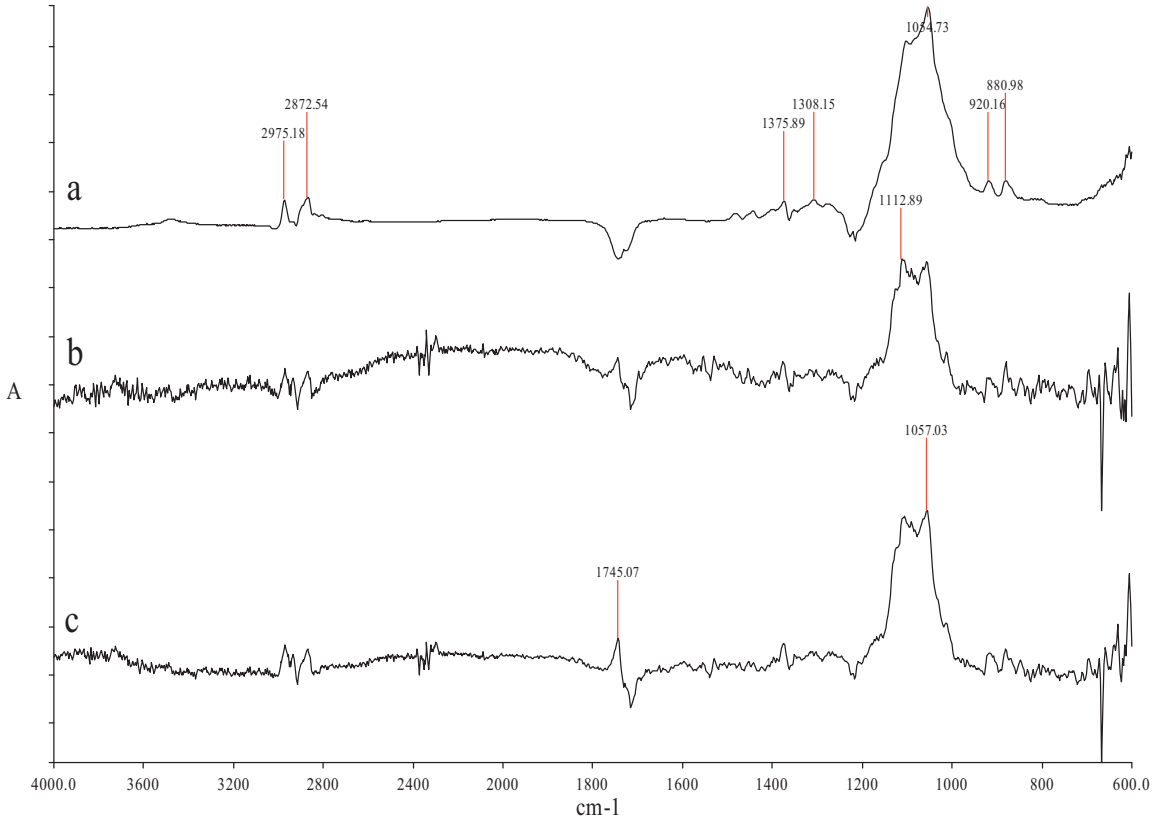

Fig. 7. FTIR spectrum of (a) ethyl cellulose powder (b) freshly made gel of 12% EC in PGD, and (c) 12% EC/PGD gel undergone prior thermal treatment.

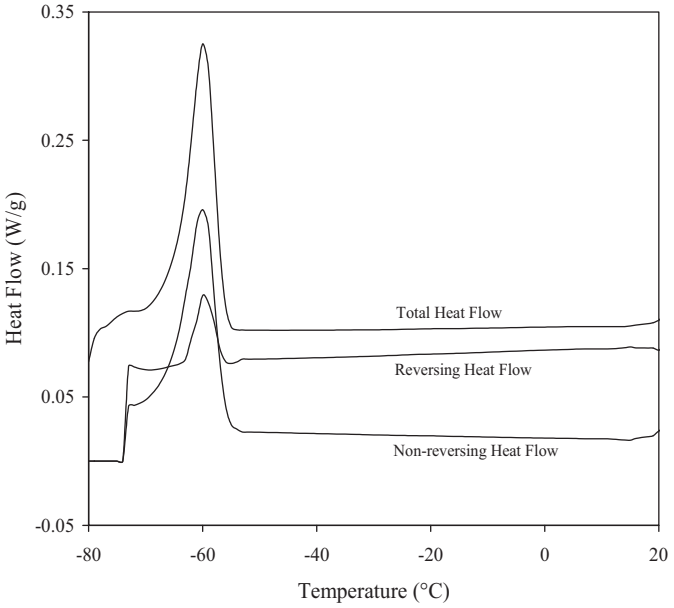

Fig. 8. Modulated DSC cooling scans of 12% EC/PGD gel or PGD solvent taken at a rate of 5 °C/min showing the total, reversing and non-reversing heat flow.

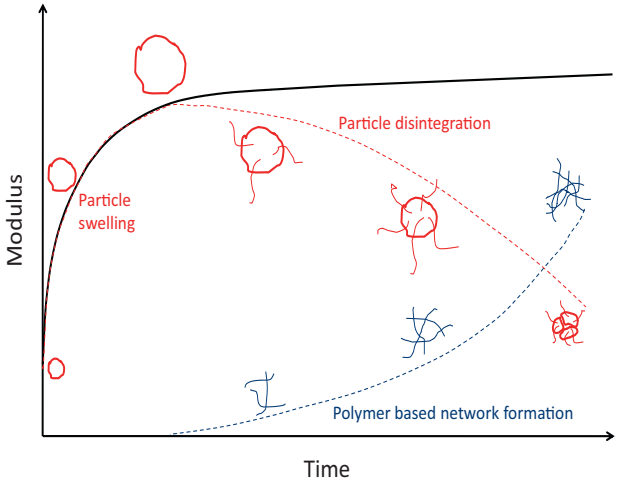

Fig. 9. Mechanistic depiction of the two molecular processes governing the structural properties of ethylcellulose/propylene glycol dicaprylate/dicaprate gel as a function of time at ambient temperature.

conspicuous in the gel where interactions of solvent molecules with chain segments generate free volume that disrupts the periodicity patterns of the polymer. This type of polymer plasticization by the PGD solvent is congruent with the rubbery state recorded for the mechanical properties of the cellulosic network in Fig. 3a.

The X-ray and infrared spectroscopy results in Figs. 6 and 7 extend conclusions drawn on the structural variation of our material subjected to an experimental isothermal or isochronic regime. The nature of the molecular processes leading to gel–sol transition with increasing temperature in Fig. 1 and structural disintegration in Fig. 4 is further discussed in this section. Since gelation of ethyl cellulose takes place with a specific physicochemical environment, the nature of polymer–solvent interactions should also be considered using micro and modulated differential scanning calorimetry.

Repeated experimentation by heating and then cooling the freshly made or a 48-h annealed gel at 25 °C (using micro DSC at a scan rate of 1 °C/min that follows the rheological protocol) failed to produce an enthalpic transition, which has been reported in the literature for thermograms of ethyl cellulose in water. Instead, only a flat baseline was recorded indicating the absence of crystallinity and associated melting peak for the non-aqueous system of this investigation within the temperature range that tan δ becomes one (viscoelastic heating profiles in Fig. 1). Besides the 12% EC/PGD system, featureless thermograms were obtained for 6% and 18% of the cellulosic derivative in preparations (results are not shown here). Following this, the temperature range of observation was extended to subzero temperatures using modulated DSC in Fig. 8 and monitoring separately the solvent solution and the mixture of polymer with solvent.

Within the temperature range of interest in this investigation (i.e. −25 °C < temp < 95 °C), total heat flow and reversing flow are virtually identical and devoid of sigmoidal patterns of heat flow that could be related to glass transition phenomena. In the absence of vitrification, there is close correspondence between this result, the master curve of viscoelasticity in Fig. 3a and the mechanistic modeling in Fig. 3b where it was argued for a soft rubbery consistency in the mechanical properties of the EC/PGD preparation spanning the temperature range of −25 °C to 5 °C. Nevertheless, thermal changes at the lower range of experimental temperatures in Fig. 8 unveil for PGD or EC/PGD two dominant cooling exotherms, which show appreciable similarity in position and shape. Thus the total heat flow and non-reversing heat flow document that the thermal event denotes primarily the freezing point of the propylene glycol dicaprylate matrix at −59 °C.

4. Conclusions

Experimental observations and quantitative treatment of results encourage us to present a sketch of the model proposed to rationalize the time effect on structural properties of the EC/PGD system (Fig. 9). The obvious interpretation of the continuous increase in viscoelasticity of the non-aqueous gel, as a function of time of observation at ambient temperature (Fig. 5), is that there are dynamic structures present in the system developing continuously. In combination with the increase in particle roughness at the initial stages of Fig. 4, which is overtaken by structural disintegration at longer periods of observation, results are suggestive of contributions from two distinct molecular processes. The passage from one process to the other should correspond to the maximum in the detectable values of particle roughness. Prior to that point, solvent diffusion and consequent particle swelling is the driving force of recorded viscoelasticity but a critical stage is reached at which partial dissociation of solvated regions will commence. As illustrated in Fig. 9, gel-forming individual strands that interact with the solvent should further underpin structure formation that is able to support particle remnants undergoing solubilisation.

Equivalence between time and temperature effects is demonstrated in the analysis of Fig. 3, which is supported by the converging patterns of structural rearrangement in EC particles with heating and prolonged aging at 25 °C in Fig. 4. This passage to temperature effects argues for direct interactions between polymer and solvent to yield specific viscoelastic profiles, X-ray diffractograms and infrared spectra for gels. On the basis of regioselectively substituted hydroxyl groups with benzyl, methyl and ethyl ether, it can been argued that the gel–sol transition observed at temperatures above 65 °C in Fig. 1b is associated with direct polymer–polymer hydrogen bonding featuring 6-position hydroxyl groups (Itagaki, Tokai, & Kondo, 1997; Kondo and Miyamoto, 1998). The second wave of structure formation observed at temperatures below 35 °C in Fig. 1a and b may involve an additional contribution from electrostatic interactions between carbonyl groups of the solvent and hydroxyl groups of the polymer.

This has been argued for EC gels using diethyl, dibutyl and di(2-ethylhexyl)phalate solvents, which produced networks with a flat frequency dependence of shear modulus on dynamic oscillation due to the formation of stable bridges between the two carbonyl groups of each diester-phalate molecule and two encompassing EC chains (Lizaso et al., 1999). Such interactions have been detected in the infrared spectra of Fig. 7, but results in Fig. 3a show a pronounced frequency dependence of shear modulus attributed to freely rotating single bonds of the dicaprylate/dicaprate backbone that reduce the efficiency of carbonyl-group polarization in EC/PGD gels. Adding to this the micro/modulated DSC results discussed in Fig. 8, it is suggested that gelation does not arise from crystallisation, is distinct from the molecular mechanisms that prevail in hydrophobic thermogelation of EC/water systems, and should be of critical importance in elucidating the functional properties of preparations related to topical drug delivery. At this stage, it is encouraging that results of the time–temperature superposition principle indicate that addition of ethyl cellulose to propylene glycol dicaprylate results in soft rubbery gels within standard conditions of ambient and near subzero temperatures for extended timescales of observation.

References

Agrawal, A. M., Manek, R. V., Kolling, W. M., & Neau, S. H. (2003). Studies on the interaction of water with ethylcellulose: Effect of polymer particle size. *AAPS PharmSciTech*, *4*, 1–11.

Alves, N. M., Mano, J. F., Gomez Ribelles, J. L., & Gomez Tejedor, J. A. (2004). Departure from the Vogel behaviour in the glass transition-thermally stimulated recovery, creep and dynamic analysis studies. *Polymer*, *45*, 1007–1017.

Arora, P., & Mukherjee, B. (2002). Design, development, physicochemical, and in vitro and in vivo evaluation of transdermal patches containing diclofenac diethylammonium salt. *Journal of Pharmaceutical Sciences*, *91*, 2076–2089.

Chan, L. W., Chow, K. T., & Heng, P. W. S. (2006). Investigation of wetting behavior of nonaqueous ethylcellulose gel matrices using dynamic contact angle. *Pharmaceutical Research*, *23*, 408–421.

Ferry, J. D. (1980). *Viscoelastic properties of polymers*. New York: John Wiley., pp. 264–320.

Ferry, J. D. (1991). Some reflections on the early development of polymer dynamics: Viscoelasticity, dielectric dispersion, and self-diffusion. *Macromolecules*, *24*, 5237–5245.

Filho, G. R., de Assuncao, R. M. N., Vieira, J. G., Meireles, C. S., Cerqueira, D. A., Barud, H. S., et al. (2007). Characterization of methylcellulose produced from sugar cane bagasse cellulose: Crystallinity and thermal properties. *Polymer Degradation and Stability*, *92*, 205–210.

Haque, A., & Morris, E. R. (1993). Thermogelation of methylcellulose. Part I: Molecular structures and processes. *Carbohydrate Polymers*, *22*, 161–173.

Heng, P. W., Chan, S., & Chow, L. W. K. T. (2005). Development of novel nonaqueous ethylcellulose gel matrices: Rheological and mechanical characterization. *Pharmaceutical Research*, *22*, 676–684.

Huang, B., Ge, J. J., Li, Y., & Hou, H. (2007). Aliphatic acid esters of (2-hydroxypropyl) cellulose—Effect of side chain length on properties of cholesteric liquid crystals. *Polymer*, *48*, 264–269.

Itagaki, H., Tokai, M., & Kondo, T. (1997). Physical gelation process for cellulose whose hydroxyl groups are regioselectively substituted by fluorescent groups. *Polymer*, *38*, 4201–4205.

Kondo, T., & Miyamoto, T. (1998). The influence of intramolecular hydrogen bonds on handedness in ethylcellulose/CH_2Cl_2 liquid crystalline mesophases. *Polymer*, *39*, 1123–1127.

Janaswamy, S., & Chandrasekaran, R. (2005). Polysaccharide structures from powder diffraction data: Molecular models of arabinan. *Carbohydrate Research*, *340*, 835–839.

Kasapis, S. (2001). The use of Arrhenius and WLF kinetics to rationalise the rubber-to-glass transition in high sugar/κ-carrageenan systems. *Food Hydrocolloids*, *15*, 239–245.

Kasapis, S. (2008). Recent advances and future challenges in the explanation and exploitation of the network glass transition of high sugar/biopolymer mixtures. *Critical Reviews in Food Science and Nutrition*, *48*, 185–203.

Kasapis, S., Al-Marhoobi, I. M., Deszczynski, M., Mitchell, J. R., & Abeysekera, R. (2003). Gelatin vs polysaccharide in mixture with sugar. *Biomacromolecules*, *4*, 1142–1149.

Kontogiorgos, V., Goff, H. D., & Kasapis, S. (2008). Effect of aging and ice structuring proteins on the morphology of frozen hydrated gluten networks. *Biomacromolecules*, *8*, 1293–1299.

Li, X. G., Kresse, I., Xu, Z. K., & Springer, J. (2001). Effect of temperature and pressure on gas transport in ethyl cellulose membrane. *Polymer*, *42*, 6801–6810.

Lizaso, E., Munoz, M. E., & Santamaria, A. (1999). Formation of gels in ethylcellulose solutions: An interpretation from dynamic viscoelastic results. *Macromolecules*, *32*, 1883–1889.

Melzer, E., Kreuter, J., & Daniels, R. (2003). Ethylcellulose: A new type of emulsion stabilizer. *European Journal of Pharmaceutics and Biopharmaceutics*, *56*, 23–27.

Nishinari, K., & Zhang, H. (2004). Recent advances in the understanding of heat set gelling polysaccharides. *Trends in Food Science and Technology*, *15*, 305–312.

Panaitescu, D. M., Donescu, D., Bercu, C., Vuluga, D. M., Iorga, M., & Ghiurea, M. (2007). Polymer composites with cellulose microfibrils. *Polymer Engineering And Science*, *47*, 1228–1234.

Puscasu, R. M., Todd, B. D., Daivis, P. J., & Hansen, J. S. (2010). Nonlocal viscosity of polymer melts approaching their glassy state. *The Journal of Chemical Physics*, *133*, 144907-(1-16).

Qiu, L. Y., & Bae, Y. H. (2006). Polymer architecture and drug delivery. *Pharmaceutical Research*, *23*, 1–30.

Raimo, M. (2007). "Kinematic" analysis of growth and coalescence of spherulites for predictions on spherulitic morphology and on the crystallization mechanism. *Progress in Polymer Science*, *32*, 597–622.

Sanchez, R., Franco, J. M., Delgado, M. A., Valencia, C., & Gallegos, C. (2011). Thermal and mechanical characterisation of cellulosic derivatives-based oleogels potentially applicable as bio-lubricating greases: Influence of ethyl cellulose molecular weight. *Carbohydrate Polymers*, *83*, 151–158.

Stenstad, P., Andresen, M., Tanem, B. S., & Stenius, P. (2008). Chemical surface modifications of microfibrillated cellulose. *Cellulose*, *15*, 35–45.

Sun, S., Foster, T. J., MacNaughtan, W., Mitchell, J. R., Fenn, D., Koschella, A., et al. (2009). Self-association of cellulose ethers with random and regioselective distribution of substitution. *Journal of Polymer Science: Part B: Polymer Physics*, *47*, 1743–1752.

Tanaka, F., & Koga, T. (2000). Intramolecular and intermolecular association in thermoreversible gelation of hydrophobically modified associating polymers. *Computational and Theoretical Polymer Science*, *10*, 259–267.

Tanaka, Y., Gong, J. P., & Osada, Y. (2005). Novel hydrogels with excellent mechanical performance. *Progress in Polymer Science*, *30*, 1–9.

Wang, L., Dong, W., & Xu, Y. (2007). Synthesis and characterization of hydroxypropyl methylcellulose and ethyl acrylate graft copolymers. *Carbohydrate Polymers*, *68*, 626–636.

Wu, P. C., Huang, Y. B., Chang, J. I., Tsai, M. J., & Tsai, Y. H. (2003). Preparation and evaluation of sustained release microspheres of potassium chloride prepared with ethylcellulose. *International Journal of Pharmaceutics*, *260*, 115–121.

Yoon, J. H., Han, J., Park, J., Choi, S., Yeon, S. H., & Lee, H. (2008). Synthesis of porous hollow silica spheres using polystyrene–methyl acrylic acid latex template at different temperatures. *Journal of Physics and Chemistry of Solids*, *69*, 1432–1437.

Zhang, Z., Zhang, H., Zhang, Q., Zhou, Q., Zhang, H., Mo, Z., et al. (2006). Thermotropic liquid crystallinity, thermal decomposition behavior, and aggregated structure of poly(propylene carbonate)/ethyl cellulose blends. *Journal of Applied Polymer Science*, *100*, 584–592.

Ziegler, I. M, Tanczos, I., Horvolgyi, Z., & Agoston, B. (2008). Water-repellent acylated and silylated wood samples and their surface analytical characterization. *Colloids and Surfaces A: Physicochemical and Engineering Aspects*, *319*, 204–212.